Advanced Powder Technology 34 (2023) 104025

Contents lists available at ScienceDirect

Advanced Powder Technology

journal homepage: www.elsevier.com/locate/apt

Original Research Paper

In depth characterisation of hydrocyclones: Ascertaining the effect of geometry and operating conditions on their performance

Javier Izquierdo [a], Xabier Sukunza [b,*], Paula Espinazo [a], Jorge Vicente [a], Roberto Aguado [b], Martin Olazar [b]

[a] Novattia Desarrollos, Ltd., Poligono Industrial Berreteaga, Txorierri Etorbidea, 46, Nave 12B, 48150, Biscay, Spain
[b] Dept. of Chemical Engineering, University of the Basque Country, UPV/EHU, PO Box 644 – E48080 Bilbao, Spain

ARTICLE INFO

Article history:
Received 19 October 2022
Received in revised form 8 February 2023
Accepted 29 March 2023
Available online 11 April 2023

Keywords:
Hydrocylones
Separation
Densification
Dewatering

ABSTRACT

Hydrocyclones are used for densification of waste streams prior to drying or for classification of solid and liquids in two-phase streams. They are becoming popular in industrial units due to their simplicity, low energy consumption and high versatility. However, the effect of geometry and operating conditions on the cut diameter and solid recovery efficiency have been independently studied, and therefore there are no studies approaching the influence of all the parameters simultaneously. Thus, a detailed experimental study was conducted to ascertain the effect of the hydrocyclone body (diameter and angle) and the vortex finder and spigot size and shape, as well as operating conditions (inlet pressure and solid concentration) on the separation efficiency curve, cut diameter, solid and volume recovery and the main features of the outlet streams. It has been proven that separation efficiency and outlet stream composition are sensitive to both the geometry of the hydrocyclone and the operating parameters. Therefore, knowledge of their influence is essential for the design of industrial units where liquid reutilisation is a major concern.

1. Introduction

The limited amount of natural resources, as well as the mandatory and urgent need for environment preservation, are currently the driving forces for a responsible use of natural resources, and therefore for minimum waste generation. Accordingly, numerous industrial processes require technologies that are efficient and of low energy consumption for the separation of two-phase liquid streams, i.e., solids suspended in a liquid stream or a stream made up of two or more immiscible liquids. Concerning the amount of liquid streams, the mining industry accounts for 7 to 14 billion tonnes [1,2]. The oil and gas industry generates from 3 to 4 barrels of wastewater from each barrel of oil extracted, with this amount being as high as 10 barrels when a well is near exhaustion [3]. Cement industry accounts for approximately 80 L of wastewater for each cubic meter of product [4] and the brewery industry for 10 L for each litre of beer produced [5]. The suitable treatment of these wastes allows reducing the environmental impact, as well as recovering interesting raw materials and promoting circular economy. Hydrocyclone technology is well established and may contribute to separating and concentrating large volumes of waste streams. Although hydrocyclones have been used for long time, new regulations involving environment preservation and the need for recovering raw materials have boosted their use in many applications. Thus, their capital and operating costs are lower than those of other equipment for the same purpose [6], and they have proven to be highly versatile in operations involving separation (desludging and desanding), classification and concentration (thickening and the recovery of solids or process water).

Hydrocyclone technology is gaining increasing attention for use in new applications, especially in those in which restrictive environmental regulations apply. Thus, Farghaly et al. [7] proposed injecting water into the conical body in order to avoid particle entrainment through the upflow stream. Hwang et al. [8] studied the effect of a conical top-plate with the aim of inducing tangential circulation, and therefore improve equipment performance. Martínez et al. [9] conducted a study to determine the optimum length of the vortex finder, and concluded that the ratio between the vortex chimney length and the whole length of the hydrocyclone must be 0.1 in order to avoid shortcuts and attain the maximum efficiency. Other studies optimized the cone angle [10,11] or the length of the conical body [12]. Although the spigot is the hydrocyclone section of easiest design, it has also been analysed in detail. Thus, Pathack et al. [13] proposed a truncated conical geometry in order to attain rope discharge in the underflow, which leads to a

* Corresponding author.
E-mail address: xabier.sukunza@ehu.eus (X. Sukunza).

https://doi.org/10.1016/j.apt.2023.104025

Nomenclature

d_p	Particle size, L	Q_o	Liquid flow rate of the overflow stream, L^3t^{-1}
D	Diameter of the hydrocyclone, L	$x_u\,(d_p)$	Fractional content of particles of given size in the underflow stream, dimensionless
D_i	Inlet diameter, L	$x_o\,(d_p)$	Fractional content of particles of given size in the overflow stream, dimensionless
L	Length of the hydrocyclone, L	R	Solid recovery efficiency, dimensionless
l	Length of the vortex chimney, L	R_v	Volumetric recovery index, dimensionless
l_c	Length of the conical section of the hydrocyclone, L	η	Separation efficiency, dimensionless
θ	Angle of the cone, dimensionless	Δp	Pressure drop, $ML^{-1}t^{-2}$
D_u	Diameter of the spigot, L	S	Inlet section, L
D_o	Diameter of the vortex finder, L	P	Inlet perimeter, L
C_f	Inlet solid concentration, ML^{-3}	d_{50}	Cut diameter, L
Q_f	Inlet liquid flow rate, L^3t^{-1}	d_{p90}	90% of the particles are similar to or smaller than d_p, L
C_u	Solid concentration of the underflow stream, ML^{-3}		
Q_u	Liquid flow rate of the underflow stream, L^3t^{-1}		
C_o	Solid concentration of the overflow stream, ML^{-3}		

higher concentration of solids (even 25% wt higher). Silva et al. [14] and Salvador et al. [15,16] proposed a hydrocyclone with a filtering conical body, which allows improving efficiency, as well as obtaining a third water stream that may be fed back into the process itself. The main disadvantage of this design lies in its cost, as bronze particles were used for the active layer of the filtering medium.

Numerous papers propose the application of these devices in operations in which standard cyclones are not suitable. Thus, Ma et al. [17] designed a hydrocyclone of 100 mm in diameter for retaining the coke powder generated in refineries, which allowed attaining 99% efficiency in the recovery of 100 μm particles. The review by Yang et al. [18] and the study by Lee [19] are evidence of the potential of hydrocyclones for the treatment of waste water. Furthermore, studies have been conduced with the aim of exploring the use of hydrocyclones for the recovery of lubricants, refrigerants, cutting oils [20], and catalysts [21]. Saengchan et al. [22] studied the performance of these devices in food industry, and other researchers have proven they are suitable for starch concentration [23,24]. A novel recent use of hydrocyclones is related to microplastic recovery [25]. Thus, He et al. [26] proposed double-inlet hydrocyclones of diameter smaller than 15 mm, which allowed recovering up to 50% of polymeric microparticles in aqueous streams. In a recent study by González Pérez et al. [27], ultrasound assisted hdydrocyclones were tested in the production of cobalt by electrolysis, with the hydrocyclone body being the cathode and the vortex finder the anode. They have proven that ultrasound assistance maintains clean the cathode surface, thus improving the yield to 58.3%.

Numerous studies have been reported in the literature concerning the use of these devices [28,29]. For instance, the effect of isolated parameters, such as the body diameter [30], vortex finder diameter [31,32], cone angle [33,34] or the spigot diameter [35–37] have been reported. There are also studies dealing with the effect of the operating pressure [38–40]. Nevertheless, to our knowledge, there are hardly any studies approaching the influence of all the parameters simultaneously. Accordingly, a detailed study has been conducted in order to identify the effect of operating conditions (pressure, feed composition and concentration of suspended solids) and hydrocyclone geometry (diameter of the body, vortex finder and spigot, and vortex finder configuration) on the performance of hydrocyclones. The output parameters analysed are the usual ones related to efficiency (size cut and particle recovery), as well as those characterizing the outlet streams (concentration of solids, volume recovery and particle size distribution in the overflow stream).

2. Experimental

2.1. Materials and equipment

Silica sand and kaolin were selected for the experimental runs. Both materials were collected from the streams in silica and kaolin production plants. Fig. 1 shows the particle size distribution of both materials, which was determined by laser diffraction in a Mastersizer 2000. The Sauter mean diameter of the silica sand and kaolin are 68.5 μm and 9.6 μm, respectively. Particle density was measured with a pycnometer and distilled water following ISO 18753:2017 standard, with the values being 2560 and 2445 kg m^{-3} for silica sand and kaolin, respectively. Given that the solid concentration may fluctuate in the mining industry processes, two different solid concentrations were tested, i.e., 35 and 75 g L^{-1} (3.4 and 7.2 wt%). These values were selected as they are currently used in mining processing plants.

Fig. 2 shows the experimental unit used for the experimental runs, and all the details corresponding to its design, construction and tuning have already been reported [41]. The pilot plant allows closed-loop operation and consists of a stirred tank for feedstock preparation (TK-1) and another one for pump feeding (TK-2), two positive displacement pumps (one for high flow rates under low

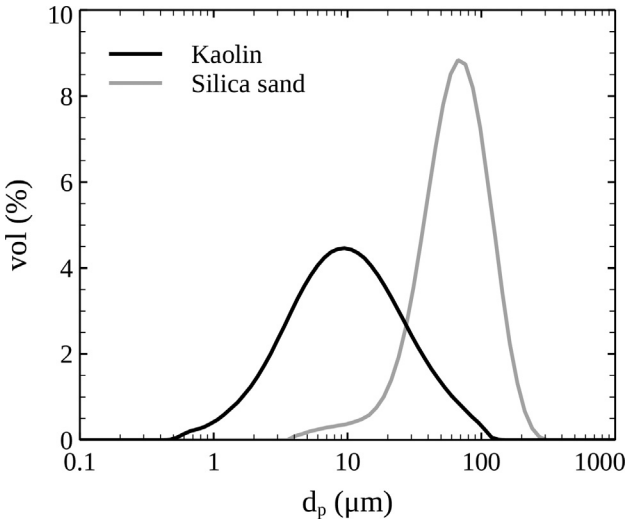

Fig. 1. Particle size distribution of silica sand and kaolin.

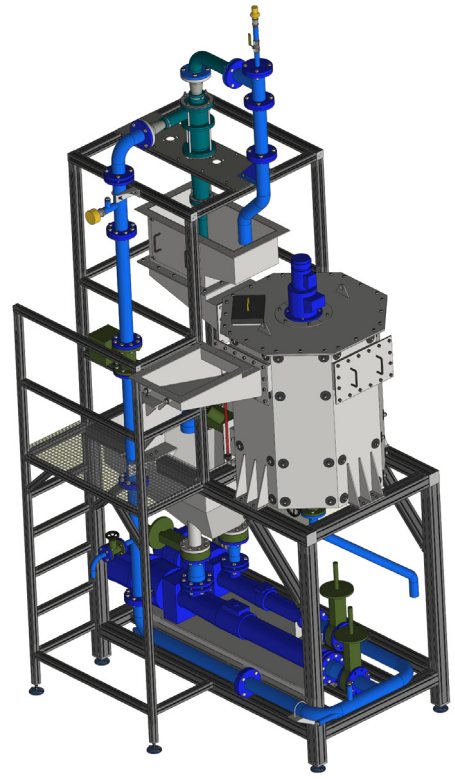

(a)

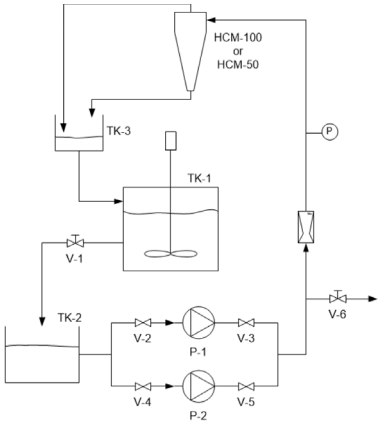

(b)

Fig. 2. (a) 3D representation of the pilot plant and (b) its corresponding flow sheet.

pressures (P-1) and the other one for low flow rates under high pressures (P-2)), the hydrocyclone for solid separation and a vessel for sample retrieval (TK-3).

The stirred tank, TK-1, of octagonal shape, is made of stainless steel, and has a maximum capacity of 700 L. An stirrer with S-type helical axial blades operated at 350 rpm to avoid solid sedimentation. Another vessel is located above this tank, which allows recirculating the overflow and underflow streams leaving the hydrocyclone. A manual DN-100 valve is located at the lower end of the tank for discharging the stream from TK-1 into the vessel feeding the recirculation pumps, TK-2. The discharge pipe from this vessel is diverted into two ones, one providing low flow rates at high pressure by means of pump P-1 and the other high flow rates at low pressure by means of pump P-2. Both pipes are provided with DN-80 guillotine valves. P-1 is a 7.5 kW positive displacement pump (Sydex BK 065-1L), which provides a nominal flow rate of 20 m^3h^{-1} at 2 bar, although it may also operate up to 5 bar. In order to operate at higher nominal pressures, a 2.2 kW positive displacement pump, P-2 (Sydex BK 039-2S), was inserted. Its nominal flow rate is 2 m^3h^{-1} at 2 bar, but it may also operate up to 12 bar. The liquid flow rate was measured by a electromagnetic flow meter (Promag 55S) supplied by Endress-Hausser Ltd. Its nominal diameter is DN-80 and the measured flow rates ranged from 0 to 300 m^3h^{-1}. The pressure transmitter (Cerabar M PMP51), also supplied by Endress-Hausser Ltd., allows measuring the pressure of the feeding stream in a range from 0 to 16 bar. The pilot plant is controlled by a LabView card, which allows controlling the rotational speed of the pumps (P-1 and P-2) and stirrer (TK-1). Furthermore, it allows collecting data of both the stream flow rate and pressure every second in order to visualise their evolution with time.

Given that the main objective of this work was to study in detail the performance of the hydrocyclones in order to determine their optimum geometry for given separation specifications, the pilot plant was designed to easily replace these device. The hydrocyclones tested were assembled combining three elements, namely, body, vortex finder and spigot, all of them made of polyurethane to avoid particle abrasion, and supplied by Novattia Desarrollos, Ltd. Accordingly, three different body geometries have been assayed, one of 100 mm in diameter, D, called HCM-100, and two of 50 mm in diameter, called HCM-50A and HCM-50B, with their main difference being in total length. Several combinations of vortex finder and spigot (differing in their diameters D_o and D_u) were tested with each body. Fig. 3 and Table 1 show the combinations of body, vortex finder and spigot used, which account for 46 different hydrocyclones studied. The inlet section of the hydrocyclones is of rectangular shape and its diameter, D_i, was estimated assuming an equivalent diameter, $4S/P$, with S being the cross-sectional area of the inlet and P its perimeter. Based on the results reported by Hwang et al. [42] and Martinez et al. [43], several vortex finder configurations have been studied, as are a standard one, Fig. 4(a), a conical one with the smaller diameter connected to the body,

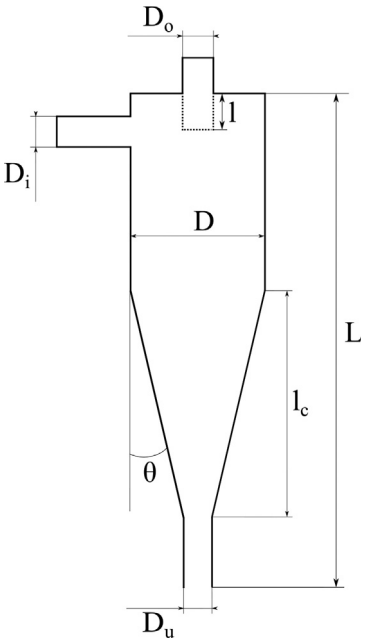

Fig. 3. Geometric parameters of the hydrocyclone.

Table 1
Features of the hydrocyclones tested.

Parameter	HCM-100	HCM-50A	HCM-50B
D, mm	100	50	50
D_i, mm	28	11	11
L, mm	1100	515	750
l, mm	95	35	35
θ, °	7.6	12.1	5.0
l_c, mm	700	200	400
D_o, mm	20, 25, 30, 40	10, 14, 18	10, 14, 18
D_u, mm	6, 8, 10, 12, 14, 16, 18	3, 6, 9	3, 6, 9

Fig. 4(b), a narrower than the standard one, Fig. 4(c), a longer than the standard one, Fig. 4a longer and narrower than the standard one, Fig. 4.

2.2. Experimental procedure

Prior to every experimental run, the pulp with the desired concentration of solids was prepared. For example, a volume of 500 L of pulp with a solid concentration of 75 g L^{-1} required 484 L of water and 37.5 kg of solids. Thus, the water was poured into the stirred tank, TK-1, the stirrer was started and the amount of solids was then added. The pulp was stirred for at least 30 min to avoid dead zones and ensure total homogenization. At the same time as stirring proceeded, the body, vortex finder and spigot were assembled and the hydrocyclone was placed in the upper section of the pilot plant. The valves were then opened and the corresponding pump (P-1 or P-2) switched on at the minimum pressure the hydrocyclone could operate. After waiting 5 min for stabilisation, the flow rate and pressure were registered and samples were collected from the underflow and overflow streams. Afterwards, pressure was increased and the process was repeated until the maximum pressure was attained. Once the runs were finished, the pump was turned off and the valves closed. The same procedure was repeated for each configuration. Prior to using a new pulp, the stirred tank was emptied and the whole unit cleaned up. In order to ascertain the performance of each configuration, pressure, flow rate, solid concentration and particle size distribution of the inlet and outlet (overflow and underflow) streams were measured. The inlet flow rates and pressures were monitored in all runs. The flow rates of the outlet stream were calculated based on mass balances for the fluid and solid, Eq. 1 and Eq. 2:

$$Q_f = Q_o + Q_u \tag{1}$$

$$Q_f C_f = Q_o C_o + Q_u C_u \tag{2}$$

where Q_f, Q_o and Q_u are the flow rates corresponding to the inlet, overflow and underflow streams, respectively, and C_f, C_o and C_u are the corresponding solid concentrations, which are determined by weighting the amount of solids and water in the sample. Accordingly, centrifugation of the sample during 8 min at 3100 rpm was carried out. Water was then removed and the remaining moisture was evaporated in a stove for 24 h at 105 °C. Cyclone separation efficiency for a given size range is defined as the amount of material within this range (wt%) recovered from the inlet stream. Given that the underflow stream is taken as reference in hydrocyclones, the separation efficiency for a given size range (d_p average size) is calculated as follows:

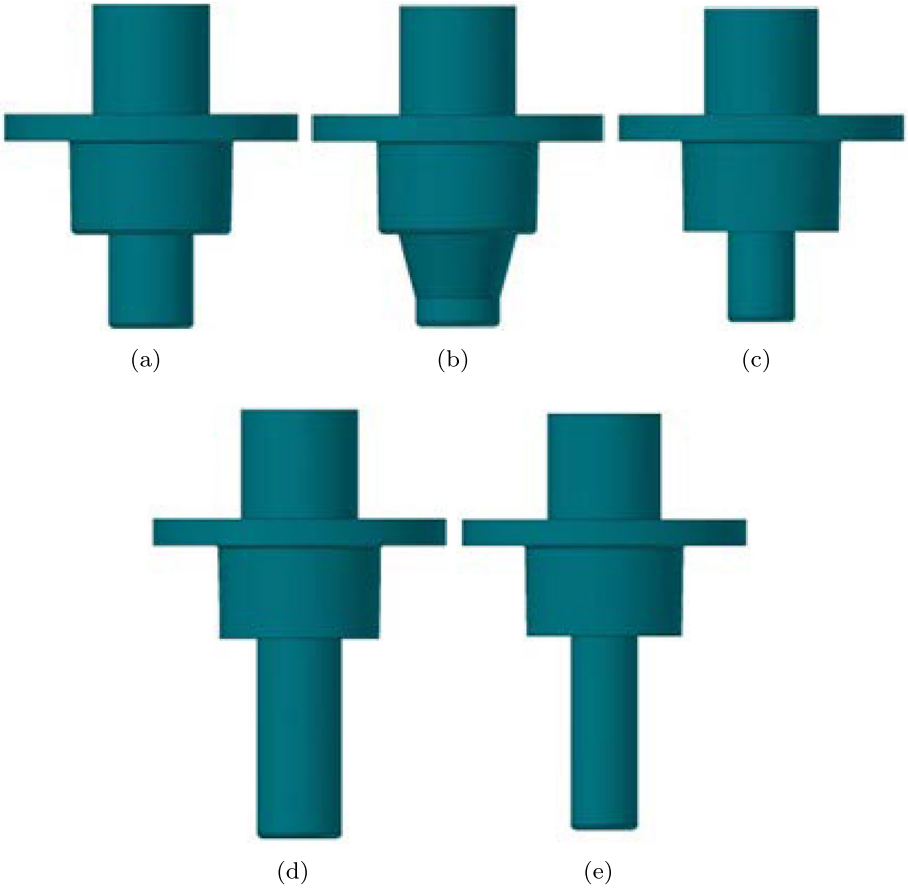

Fig. 4. Vortex finder geometries used, (a) standard, (b) conical, (c) narrow, (d) long and (e) long and narrow.

$$\eta(d_p) = \frac{Q_u C_u x_u(d_p)}{Q_u C_u x_u(d_p) + Q_o C_o x_o(d_p)} \tag{3}$$

where $x_o(d_p)$ and $x_u(d_p)$ stand for the fraction of particles of size d_p in the overflow and underflow streams, which were determined by laser diffraction in a Mastersizer 2000. Another two parameters that shed light on the separation performance are the solid recovery efficiency, R, and volume recovery, R_v, Eqs. 4 and 5, respectively:

$$R = \frac{Q_u C_u}{Q_f C_f} \tag{4}$$

$$R_v = \frac{Q_u}{Q_f} \tag{5}$$

Eq. 4 was first defined by Chu et al. [44], and relates the solid flow rate in the underflow stream with that in the inlet stream. Eq. 5 allows calculating the fraction of the inlet stream flow rate leaving through the underflow stream [45–47].

3. Results and discussion

Capacity and separation efficiency curves are the most widely extended way to describe hydrocyclone performance. The former shows the evolution of flow rate with pressure drop and allows ascertaining the minimum number of devices in parallel required for treating a certain stream. Empirical correlations relating this pair of variables have been proposed elsewhere [41]. Efficiency curves, also known as Tromp curves, provide information of the separation efficiency by relating the underflow stream with particle diameter, and they allow selecting the best hydrocyclone for a certain purpose. This study deals with the effect of operating conditions, namely, inlet pressure, concentration of solids and their properties, as well as hydrocyclone geometry, on the efficiency of the separation process. Table 1 shows the most representative features of the 46 hydrocyclones analysed in this study.

3.1. Effect of operating conditions

Fig. 5 shows the effect of the inlet pressure on the separation efficiency for two representative combinations of the geometric parameters, as are (i) $D = 100$ mm, $D_o = 30$ mm and $D_u = 6$ mm, Fig. 5ii) $D = 50$ mm, $D_o = 14$ mm, $D_u = 6$ mm and $\theta = 12°$, Fig. 5 (b). Overall, the separation performance of the hydrocyclone is sensitive to the inlet pressure. Thus, it is improved at high inlet pressures, as the efficiency curve shifts to the left. This is closely related to the values of the cut diameter, d_{50}, i.e., the particle size that has the same probability of exiting through the overflow and underflow, which is smaller as the inlet pressure is increased. This is explained by the centrifugal force exerted on the particles. As the inlet pressure is increased, the centrifugal force on the particles also increases. Therefore, both the coarse and the fine fraction of the solid entering into the hydrocyclone are more likely to be displaced onto the inner wall of the cyclone, thus increasing the amount of fine particles in the underflow stream [44,45,48–51].

Likewise, the value of the solid recovery efficiency, Eq. 4, increases as the inlet pressure is increased for all the hydrocyclones tested. Fig. 6(a) shows the evolution of solid recovery efficiency with inlet pressure for the same two hydrocyclones whose results are shown in Fig. 5. As observed, R is improved about 50% when the inlet pressure is 4 times higher. Another parameter established for ascertaining the hydrocyclone separation efficiency is d_{p90} in the overflow stream, i.e., the biggest particle size in the 90% volume fraction of the particles leaving the hydrocyclone in that stream. This parameter provides an indication of the overall quality of the overflow. As shown in Fig. 6(b), corresponding to

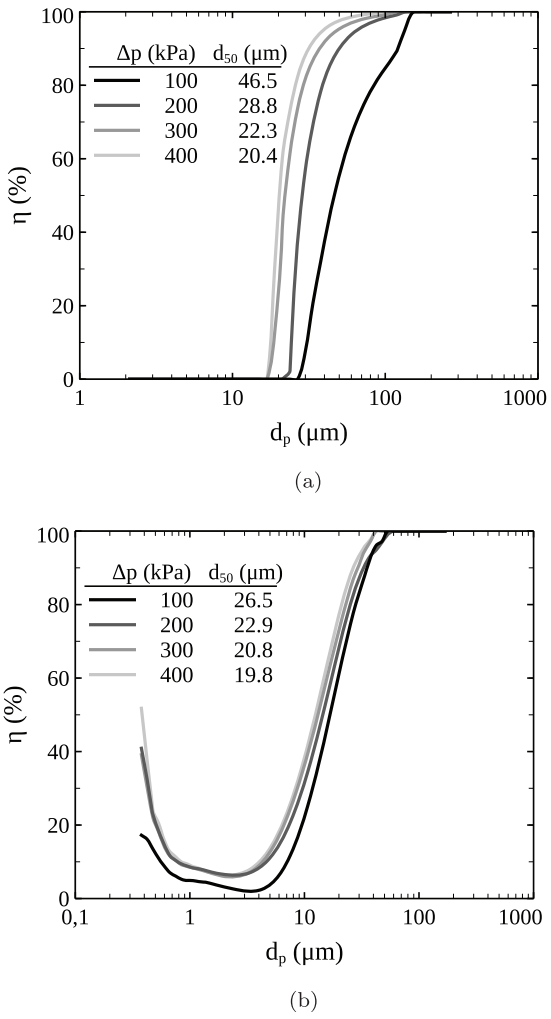

Fig. 5. Effect of the inlet pressure on the separation efficiency in two representative hydrocyclones, a) $D = 100$ mm, $D_o = 30$ mm and $D_u = 6$ mm, and b) $D = 50$ mm, $D_o = 14$ mm, $D_u = 6$ mm and $\theta = 12°$.

the same two hydrocyclones in Fig. 5, as the inlet pressure is increased the amount of coarse particles in the overflow stream decreases, i.e., the separation efficiency and overflow quality are improved.

Although the concentrations of the overflow and underflow streams are not usually considered for determining hydrocyclone separation efficiency, they are analysed in detail in this study due to their significance in the design of downstream equipment in industry. It should be noted that an increase in the separation efficiency does not necessary involve an increase in the concentration of the underflow; that is, the liquid volume may also increase apart from the amount of particles. In fact, the type of discharge in the underflow stream has an influence in dilute feeds like those used in this study. Therefore, knowledge of volume recovery, Eq. 5, is also essential apart from the concentration of the outgoing streams. These results are shown in Fig. 7 for two hydrocyclones of $D = 100$ mm with different types of discharges: one of $D_o = 30$ mm and $D_u = 6$ mm with rope discharge, and the other one of $D_o = 20$ mm and $D_u = 18$ mm with spray discharge. Overall, when spray discharge occurs, i.e., no particle accumulation in the spigot, the solid concentration in the overflow and underflow streams decreases when the inlet pressure is increased, Figs. 7(a) and 7 (b), due to the increase in the volume recovery when the inlet pressure is increased, Fig. 7(c). Nevertheless, when rope discharge occurs, i.e., particle accumulate in the spigot, the solid concentra-

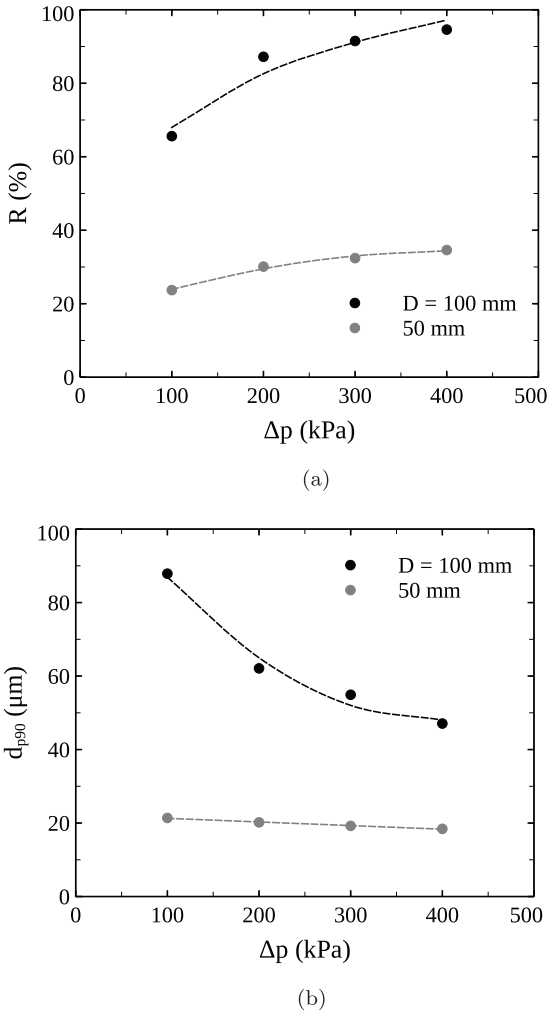

Fig. 6. Effect of the inlet pressure on a) solid recovery efficiency and b) d_{p90} of the overflow stream, in two representative hydrocyclones ($D = 100$ mm, $D_o = 30$ mm and $D_u = 6$ mm, and $D = 50$ mm, $D_o = 14$ mm, $D_u = 6$ mm and $\theta = 12°$).

tion in the underflow stream, as well as the volume recovery increase slightly as inlet pressure is increased, Figs. 7(b) and 7(c), respectively, whereas the solid concentration in the overflow stream decreases in a very pronounced way, Fig. 7(a). These results are consistent with those reported by Narashima et al. [52] and Zhang et al. [53].

Another parameter that may affect the separation efficiency is the solid concentration in the inlet stream, which may fluctuate due to the changing performance of upstream equipment in industrial facilities. Fig. 8 shows the effect of the inlet solid concentration on the separation efficiency and cut diameter in two hydrocyclones differing in the size of the vortex finder ($D = 100$ mm and $D_u = 6$ mm and vortex finder diameters of $D_o = 20$ mm, Fig. 8a) and and $D_o = 40$ mm, Fig. 8(b)). Overall, when the vortex finder diameter is small, the solid concentration in the inlet stream does not affect significantly the hydrocyclone performance, as both separation efficiency and cut diameter are similar regardless of the inlet solid concentration. However, operation with a large vortex finder and high inlet solid concentration shifts the separation efficiency curve to the right, i.e., lower separation efficiency. This is explained mainly by the role played by the diameter of the vortex ascending through the core of the cyclone. According to Davailles et al. [54] and Saengchan et al. [51], an increase in the diameter of the vortex finder leads to an increase in the diameter of the ascending vortex. This enhances particle entrainment through

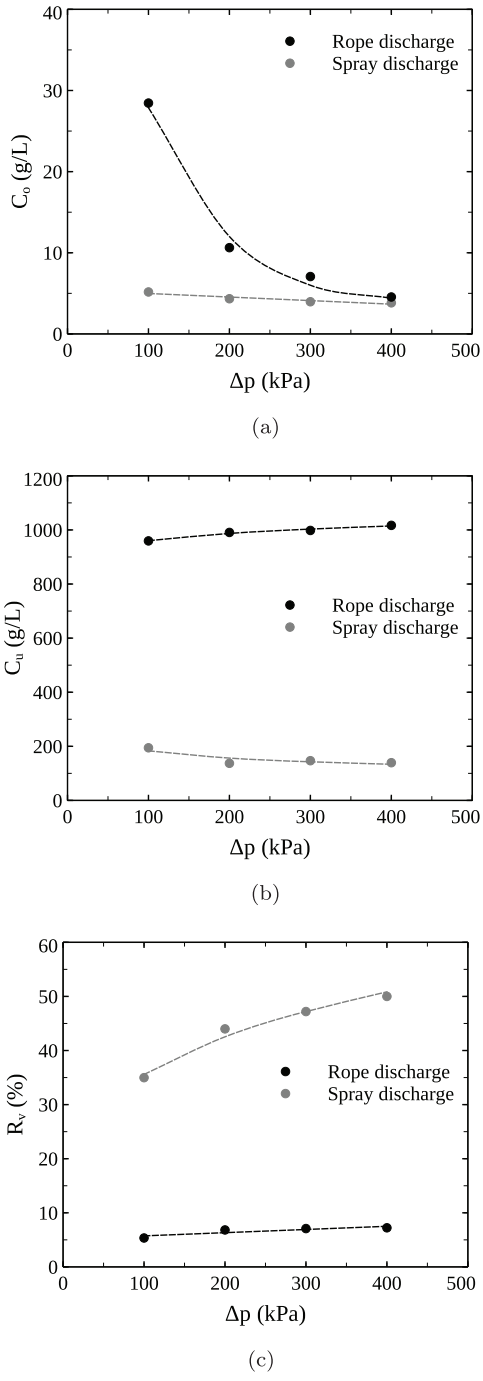

Fig. 7. Effect of the inlet pressure on (a) solid concentration in the overflow stream, (b) solid concentration in the underflow stream and on (c) volume recovery for rope discharge ($D = 100$ mm, $D_o = 30$ mm, $D_u = 6$ mm) and spray discharge ($D = 100$ mm, $D_o = 20$ mm, $D_u = 18$ mm).

the overflow stream, and therefore the amount of particles dragged through the overflow increases, with this effect being more pronounced when the inlet concentration is increased [45,55].

Fig. 9 shows the effect of solid concentration on d_{p90} in the hydrocyclone corresponding to Fig. 8(b) ($D = 100$ mm, $D_o = 40$ mm and $D_u = 6$ mm). As shown, the value of d_{p90} decreases when reducing the inlet concentration. These results are consistent with those shown in Fig. 8(b), since the quality of the overflow stream improves as the inlet pressure is increased and solid concentration is decreased.

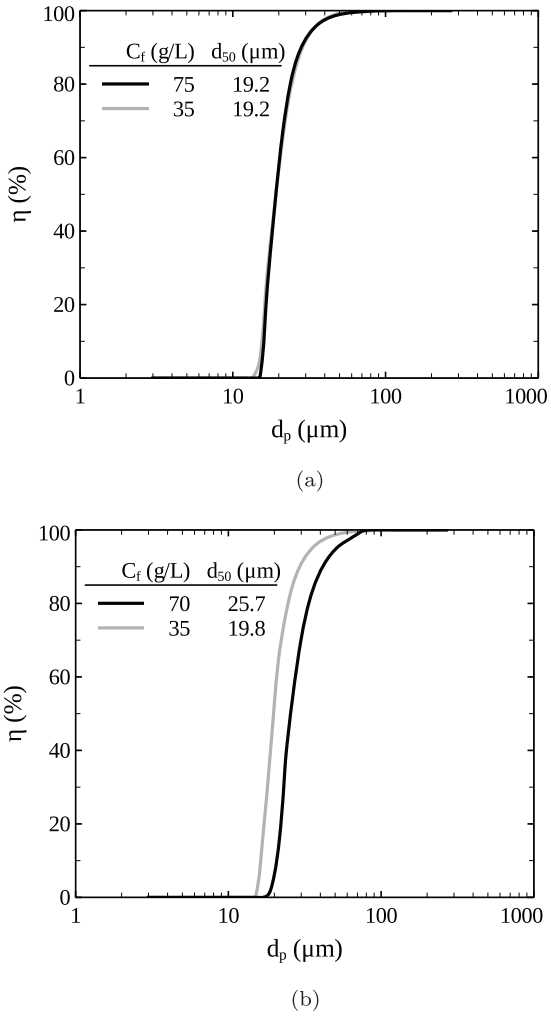

Fig. 8. Effect of the solid concentration in the inlet stream on the separation efficiency. Δp = 200 kPa, $D = 100$ mm and $D_u = 6$ mm. (a) $D_o = 20$ mm and (b) $D_o = 40$ mm.

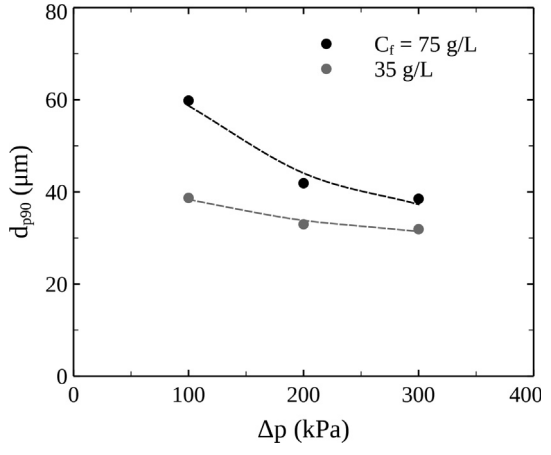

Fig. 9. Effect of inlet pressure and solid concentration in the inlet stream on d_{p90}. $D = 100$ mm, $D_o = 40$ mm and $D_u = 6$ mm.

Fig. 10 shows the separation efficiency curves when silica sand and kaolin are used in a hydrocyclone of $D = 100$ mm, $D_o = 40$ mm and $D_u = 6$ mm with an inlet pressure of 300 kPa. Overall, although the cut diameter is similar for both materials, the separation efficiency is higher for the material of higher density, i.e., silica sand ($\rho = 2560$ kg m^{-3}). Moreover, hydrocyclones perform better with coarse and spherical particles [56,57], such as those of silica sand in this study. Fig. 11 shows the evolution of solid concentration in the underflow and overflow streams for the two solids when

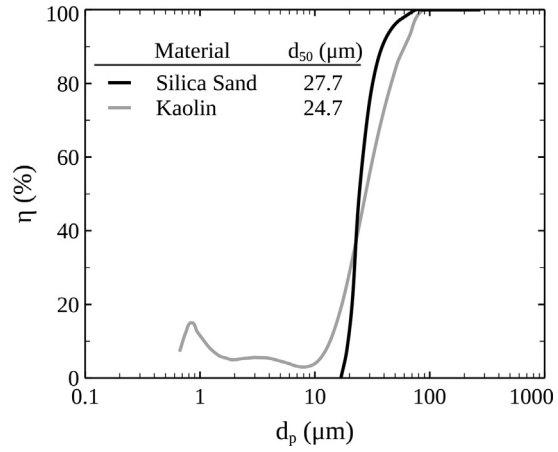

Fig. 10. Separation efficiency curves using silica sand and kaolin. $D = 100$ mm, $D_o = 40$ mm, $D_u = 6$ mm and $\Delta p = 300$ kPa.

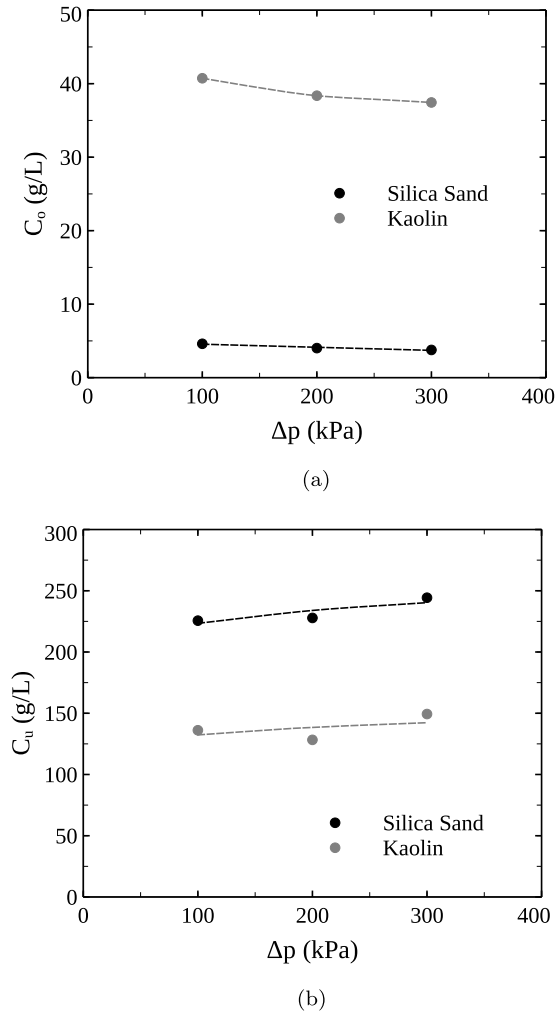

Fig. 11. Effect of the inlet stream properties on the solid concentration in the outlet streams, a) overflow and b) underflow. $D = 100$ mm, $D_o = 20$ mm and $D_u = 14$ mm.

the inlet pressure is increased from 100 kPa to 300 kPa. Given that a slightly higher separation efficiency was attained when operating with silica sand, Fig. 11 allows inferring that most of the particles are dragged into the underflow stream. Thus, the overflow stream is very dilute when operating with this material, Fig. 11(a). However, given the laminar morphology of kaolin particles and their smaller mean size than those of silica sand, the concentration of kaolin particles dragged through the overflow stream is considerably higher than that of sand particles. This involves a lower solid separation efficiency of the hydrocyclone when kaolin was used, i.e., a lower concentration in the underflow stream, Fig. 11(b).

3.2. Effect of geometric parameters

The main drawback of hydrocyclones lies in their lack of versatility, as they are designed for specific operating conditions used in certain industrial process. Thus, the performance of hydrocyclones drastically changes when the features of the upstream (solid concentration, flow rate or pressure) fluctuate. This problem is commonly attenuated by modifying the geometry of any of the parts of the hydrocyclone, i.e., body, vortex finder or spigot. Among them, the spigot is the most available and cheapest part for changing, as its diameter, D_u, is commonly modified to adapt the device to new operating conditions. However, the vortex finder geometry (diameter and chimney shape) and the body cone angle, θ, have also been analysed in this study. Fig. 12 shows the separation efficiency curves of two hydrocyclones provided with spigots of different diameters. Fig. 12(a) shows the results corresponding to a device of $D = 100$ mm and $D_o = 40$ mm operated at an inlet pressure of 300 kPa, and Fig. 12(b) those corresponding to another hydrocyclone, whose geometric factors are $D = 50$ mm, $D_o = 10$ mm and $\theta = 5°$, which was operated at an inlet pressure of 200 kPa. Overall, an increase in spigot diameter enhances the separation efficiency. This conclusion can be extended to all geometries tested. Accordingly, large diameter spigots allow feeding higher flow rates at the same pressure drop, and therefore the amount of particles leaving the hydrocyclone through the underflow stream increases [45,51,54,58,59,14]. The solid recovery efficiency, R, is also improved when operating with large diameter spigots. Thus, the results obtained with the hydrocyclone corresponding to Fig. 12(a) show that this parameter increases from 86.1% to 92.0% when the spigot diameter changes from 6 to 16 mm. Operating at 200 kPa with the hydrocyclone of smallest body ($D = 50$ mm, $\theta = 5°$ and vortex finder diameter of 10 mm) leads to an increase in the value of the solid recovery efficiency from 40.1% to 56.3% when the spigot diameter is increased from 3 to 9 mm, Fig. 12(b).

The overall quality of the overflow stream, which is determined by d_{p90} parameter, is also sensitive to the spigot diameter. Table 2 sets out the measured values of d_{p90} when operation was carried out with the same two hydrocyclones considered in Fig. 12, with both operating at an inlet pressure of 200 kPa. When the spigot diameter is increased from 6 to 18 mm in the bigger cyclone, the value of d_{p90} decreases from 38.5 to 25.3 μm. The decrease in d_{p90} is less significant in the smallest cyclone (from 18.6 to 15.3) when the spigot diameter is increased from 3 to 9 mm.

Although an increase in spigot diameter enhances the separation efficiency by widening the particle size distribution in the underflow stream, there is a lack of information related to the amount of liquid and solid leaving the underflow and overflow streams. Thus, Fig. 13 shows the solid concentration of the overflow and underflow streams and the volume recovery when operating at an inlet pressure of 200 kPa with a $D = 100$ mm hydrocyclone, in which two vortex finders of 20 and 40 mm in diameter have been used. As observed, the values of the three

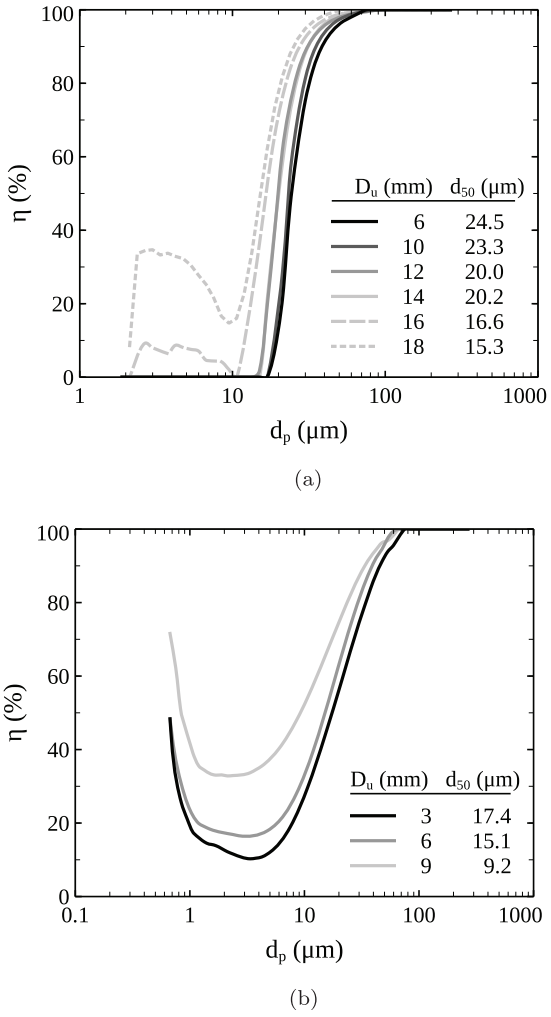

Fig. 12. Effect of the spigot diameter on the separation efficiency, a) $D = 100$ mm, $D_o = 40$ mm and $\Delta P = 300$ kPa, and b) $D = 50$ mm, $D_o = 10$ mm, $\theta = 5°$ and $\Delta p = 200$ kPa.

Table 2
Effect of the spigot diameter on the d_{p90} of the overflow stream, $\Delta p = 200$ kPa.

$D = 100$ mm, $D_o = 40$ mm		$D = 50$ mm, $D_o = 10$ mm	
D_u (mm)	d_{p90} (mm)	D_u (mm)	d_{p90} (mm)
6	38.5	3	18.6
10	37.8		
12	36.2	6	17.4
14	31.8		
16	30.6	9	15.3
18	25.3		

parameters are sensitive to the geometry of both vortex finder and spigot. Thus, an increase in the spigot diameter in a hydrocyclone with a vortex finder diameter of $D_o = 20$ mm leads to a slight increase in the solid concentration in the overflow, Fig. 13(a), but to a significant decrease in the underflow concentration, Fig. 13 (b). This is explained by the attainment of spray discharge in this configuration, which helps liquid discharge in the underflow stream. This also leads to a sharp increase in volume recovery as the spigot size (diameter) is increased, Fig. 13(c). However, when operating with a large vortex finder, $D_o = 40$ mm, the solid concentration in the overflow stream decreases and that in the underflow increases slightly when the spigot diameter is increased. Rope discharge was observed in this particular configuration, which favours

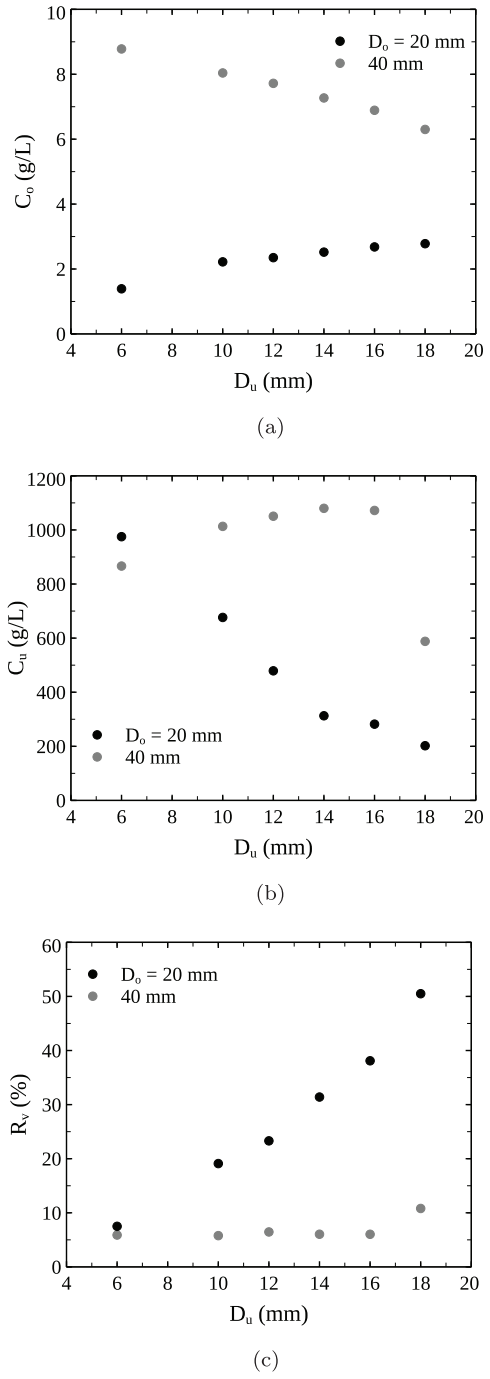

Fig. 13. Effect of the spigot diameter on (a) solid concentration in the overflow stream, (b) solid concentration in the underflow stream and (c) volume recovery. $D = 100$ mm and $\Delta p = 200$ kPa.

solid discharge in the underflow stream. Nevertheless, a sharp decrease in the solid concentration in the underflow stream was registered when the largest spigot of $D_u = 18$ mm in diameter was used, Fig. 13(b). This is explained by the change in the discharge mechanism. Thus, when operating with large spigots, the discharge mechanism shifts from rope to spray type, which, as aforementioned, leads to a decrease in the overall solid concentration of the stream, but to an increase in the volume recovery, Fig. 13(c).

Fig. 14 shows the separation efficiency curves using vortex finders differing in diameter, from 20 to 40 mm, when operation was carried out with a hydrocyclone of $D = 100$ mm and a spigot diameter (D_u) of 14 mm, at an inlet pressure of 200 kPa. Overall, the cut diameter increases as the vortex finder diameter is increased. A larger vortex finder allows treating a higher flow rate, which benefits the solid discharge in the overflow stream, and consequently the separation performance of the hydrocyclone decreases [45,59,58,60]. The solid recovery efficiency, R, also decreases as the size (diameter) of the vortex finder is increased for all the hydrocyclones studied, whose geometric factors are shown in Table 1. As an example, its value decreases from 96.1 to 89.6% in the hydrocyclones used in Fig. 14.

As aforementioned, large vortex finders promote liquid discharge through the upper outlet. Fig. 15 shows the effect of vortex finder size on the solid concentration in both outgoing streams. The results correspond to a hydrocyclone of 100 mm in body diameter and 14 mm in spigot diameter, to which vortex finders from 20 mm to 40 mm have been assembled, with operation being carried out at an inlet pressure of 200 kPa. Although an increase in vortex finder size contributes to increasing the overflow stream flow rate, the solid concentration in this stream follows a trend with an inverse peak, Fig. 15(a), whereas the solid concentration in the underflow stream increases as the size of the vortex finder is increased, Fig. 15(b). These trends are explained by the promotion of solid and/or liquid flow rates discharged through these streams depending on the configuration. Thus, as shown in Fig. 15(a), solid concentration in the overflow decreases from 4.3 to 2.7 g L^{-1} as the vortex finder diameter is increased from 20 to 25 mm, which is due to the promotion of liquid discharge through the vortex finder rather than the solid discharge. Nevertheless, a further increase in the vortex finder diameter leads to an increase in the solid concentration in the overflow stream, reaching a value of 8.3 g L^{-1} when the vortex finder is as high as $D_o = 40$ mm in diameter. It should be noted that this trend was not observed in smaller hydrocyclones, such as those with a body diameter of $D = 50$ mm, in which the solid concentration in both the overflow and underflow streams increases as vortex finder size is increased.

Fig. 16 shows the separation efficiency curve of a hydrocyclone whose dimensions are 50 mm body diameter, 18 mm vortex finder diameter, 6 mm spigot diameter and $\theta = 5$ ° cone angle, operating at an inlet pressure of 300 kPa. The vortex finder geometries used with this hydrocyclone are those described in Fig. 4meter of the vortex finder was kept constant. Overall, the shape of the vortex finder is of lower influence than other geometric parameters studied in this paper. However, the maximum separation efficiency is attained using the long (standard diameter) and the long and narrow vortex finders (Figs. 4(c) and 4(e)). Therefore, the optimum

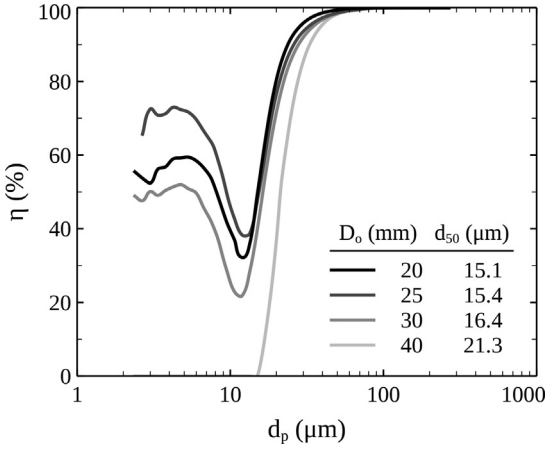

Fig. 14. Effect of the vortex finder diameter on the separation efficiency curve. $D = 100$ mm, $D_u = 14$ mm and $\Delta p = 200$ kPa.

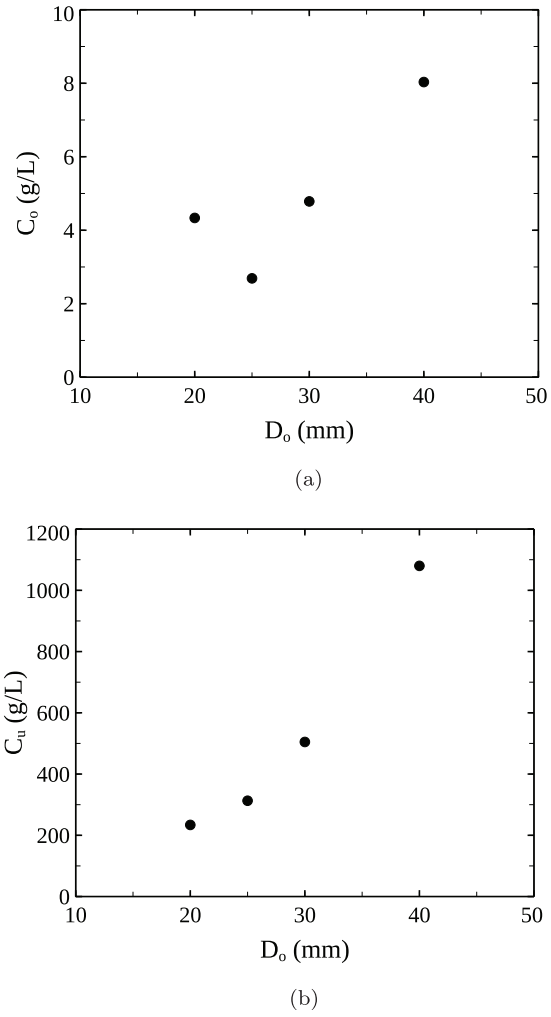

Fig. 15. Effect of the vortex finder diameter on the solid concentration in the a) overflow stream and b) underflow stream. $D = 100$ mm, $D_u = 14$ mm and $\Delta p = 200$ kPa.

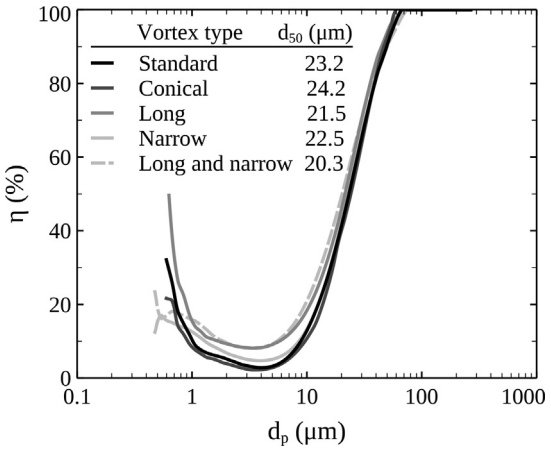

Fig. 16. Evolution of the separation efficiency curve with different vortex finder geometries. $D = 50$ mm, $D_o = 18$ mm, $D_u = 6$ mm, $\theta = 5$ ° and $\Delta p = 300$ kPa.

ratio between the length of the conical section and the total length of the hydrocyclone, l_c/L, is 0.1, which is consistent with the results reported by Martinez et al. [43]. As observed in Fig. 16, operation with the narrow vortex finder allows improving slightly the separation efficiency, as it allows decreasing the value of the cut diameter from 23.2 μm to 22.5 μm. However, operation with the vortex finder of conical shape does not improve the separation performance, which is not consistent with the results reported by Hwang et al. [42] for a body of $D = 20$ mm in diameter. Nevertheless, these authors used a silica sand of 1.75 μm Sauter mean diameter, which is lower than that of the sand used in this study. The trends shown in Fig. 16 are confirmed by the solid recovery efficiency and quality of the overflow stream obtained for kaolin separation when operation was carried out at 400 kPa with the hydrocyclone of best performance ($D = 50$ mm, $D_o = 10$ mm and $D_u = 9$ mm). Thus, the cut diameter drops from 9.5 to 7.3 μm when the standard vortex finder is replaced with the long and narrow one. Likewise, the solid recovery efficiency increases from 56.6 to 62.2 and the value of d_{p90} decreases from 14.8 to 13.4 μm. Moreover, given that the long and narrow vortex finder reduces the liquid bypass in the vortex area, and therefore increases the inlet flow development, the solid concentration in the underflow stream decreased in the 20 - 30% range.

Another geometric factor analysed in this study is the cone angle of the hydrocyclone, θ. Fig. 17 shows the separation efficiency curves for two hydrocyclones of $D = 50$ mm, $D_o = 14$ mm and $D_u = 3$ mm, operated at 200 kPa, with their cone angles being 5 and 12°. It should be noted that a smaller cone angle leads to an increase in the total length of the cyclone, which means the swirls of the vortex are more expanded along the length of the cyclone. Accordingly, the cut diameter is reduced and the overall performance of the hydrocyclone improved [47,61,62]. Thus, as the cone angle is decreased from 12 to 5°, the solid recovery efficiency increases from 19.1 to 34.7% and d_{p90} decreases from 2.02 to 18.8 μm. Moreover, a reduction in the cone angle avoids solid clogging in the spigot, thereby promoting spray discharge. Therefore, the cone angle influences the solid concentration in both the underflow and the overflow streams, with the trend in the underflow stream depending mainly on the type of discharge through the spigot. Thus, rope discharge operation leads to an increase in solid concentration when the cone angle is decreased, whereas the reverse is true for spray discharge operation. Concerning the overflow stream, solid concentration decreases when the cone angle is decreased regardless the type of discharge in the spigot.

3.3. Significant factors affecting the separation efficiency

Given that both operating conditions and hydrocyclone geometry are influential on the performance of the hydrocyclones, ascertaining the main factors and binary interactions of greatest

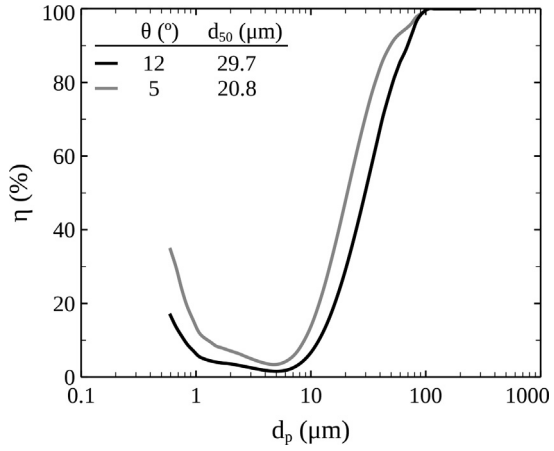

Fig. 17. Effect of the cone angle on the separation efficiency curve. $D = 50$ mm, $D_o = 14$ mm, $D_u = 3$ mm and $\Delta p = 200$ kPa.

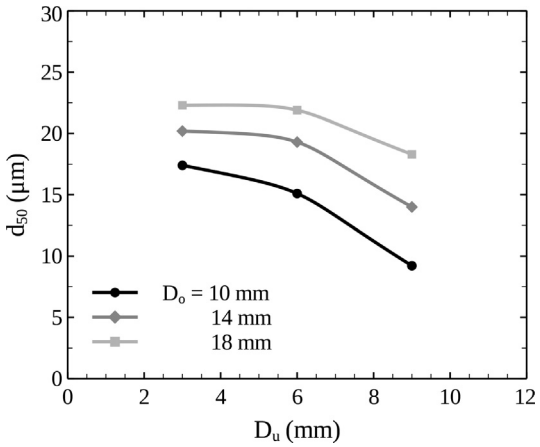

Fig. 18. Influence of the vortex finder diameter for different sizes of the spigot diameter. $D = 50$ mm, $\theta = 5°$ and $\Delta p = 100$ kPa.

influence is essential for the design of these devices. Accordingly, an analysis of variance (ANOVA) has been conducted using a standard statistical package (SPSS 28.0) and taking the cut diameter as the response variable. The statistical analysis has been applied with a 95% confidence interval. The factors used in the analysis are the size of the hydrocyclone (diameter of the body), the vortex finder diameter (D_o), the spigot diameter (D_u), the cone angle (θ), the inlet pressure (Δp), the inlet solid concentration (C_f) and the solid type (silica sand and kaolin).

The significance order of the factors analysed is as follows: $D_o > D_u \gg \theta > P \gg D_o * D_u$. The vortex finder diameter is the most influential parameter, followed by the spigot diameter, which is clearly shown in Figs. 12 and 14. Furthermore, the cone angle and the inlet pressure are also significant factors, but to a much lesser degree. As explained above, the cone angle leads to an increase in the length of the cyclone, thereby expanding the swirl of the vortex along the length of the cyclone. Moreover, an increase in the inlet pressure leads to a greater centrifugal force on the particles.

The interaction of the vortex finder diameter with the spigot diameter has also a significant effect on the cut diameter. Thus, the quantitative effect of this factor may be observed in Fig. 18. As observed in this figure, the cut diameter decreases as the diameter of the vortex is decreased. However, this reduction is more significant when large spigot diameters are used than when small ones are used, which suggest that the size of both the vortex finder and the spigot (optimum combination) should be considered in the design of industrial units.

4. Conclusions

The performance of a wide range of hydrocyclones differing in their geometry was studied under different operation conditions (inlet pressure, and solid concentration and properties). The separation efficiency curve, cut diameter, solid and volume recovery, as well as the main features of the outlet streams were also determined. An increase in the inlet pressure enhances the separation efficiency, since the cut diameter decreases, and both the solid recovery and the overall quality of the overflow stream increase. This is explained by the increase in the centrifugal force exerted on the particles in the cyclone when the inlet pressure is increased. However, the effect of the inlet solid concentration depends mainly on the hydrocyclone configuration, since the ascending vortex in the cyclone depends on the geometry of the hydrocyclone. Accordingly, operating with large vortex finders and spigots lead to high ascending vortex diameters, thereby enhancing particle entrainment. Low inlet solid concentrations in these configurations lead to a high separation efficiency, as the entrainment probability of coarse particles through the overflow stream decreases. This effect was not observed with small vortex finders and spigots, since the size of the ascending vortex is much smaller.

The geometric features of the hydrocyclones also contribute to the separation efficiency of the cyclones. Accordingly, an spigot of larger diameter enhances the hydrocyclone performance, as the pressure drop in the spigot is reduced, and therefore the solid discharge through this outlet is favoured. However, an increase in the diameter of the vortex finder leads to a reduction in the separation efficiency, since it contributes to increasing the size of the ascending vortex. Furthermore, different vortex finder geometries were tested. Concerning the length of the vortex finder, it has a great influence on the hydrocyclone performance. Thus, an increase in this dimension greatly improves separation efficiency. Nevertheless, conical vortex finders hardly affect the hydrocyclone performance. Regarding the angle of the hydrocyclone body, a reduction in the angle involves a longer body, which leads to the expansion of the vortex swirls, and therefore to a better separation performance.

The factors of greatest influence and their significance order on the cut diameter have been ascertained by conducting an analysis of variance (ANOVA). The vortex finder diameter and the spigot diameter are the most influential parameters, followed by the cone angle, the inlet pressure and the interaction of the vortex finder diameter with the spigot diameter. Therefore, the best separation performance is attained by using hydrocyclones with small vortex finder diameters, large spigot diameters and long cyclone body lengths (small cone angles), operating at high inlet pressures. Accordingly, the results obtained in this study suggest that these parameters should be considered in the design of industrial units where liquid reutilisation is a major concern.

Declaration of Competing Interest

The authors declare that they have no known competing financial interests or personal relationships that could have appeared to influence the work reported in this paper.

Acknowledgements

This work has been carried out with the financial support from the University of the Basque Country UPV/EHU (Projects US12/11 and US16/26) and the collaboration of Novattia Desarrollos Ltd. Javier Izquierdo thanks the University of the Basque Country UPV/EHU for his Ph.D. grant. Xabier Sukunza thanks the Ministry of Economy and Competitiveness for his Ph.D. grant (FPU18/04935).

References

[1] H. Jones, D.V. Boger, Sustainability and waste management in the resource industries, Ind. Eng. Chem. Res. 51 (30) (2012) 10057–10065, https://doi.org/10.1021/ie202963z.
[2] M. Edraki, T. Baumgartl, E. Manlapig, D. Bradshaw, D.M. Franks, C.J. Moran, Designing mine tailings for better environmental, social and economic outcomes: A review of alternative approaches, J. Clean. Prod. 84 (1) (2014) 411–420, https://doi.org/10.1016/j.jclepro.2014.04.079.
[3] J. Minier-Matar, M. Al-Maas, A. Hussain, M.S. Nasser, S. Adham, Pilot-scale evaluation of forward osmosis membranes for volume reduction of industrial wastewater, Desalination 531 (2022) 115689, https://doi.org/10.1016/j.desal.2022.115689.
[4] X. Chen, J. Wu, Y. Ning, W. Zhang, Experimental study on the effect of wastewater and waste slurry of mixing plant on mechanical properties and microstructure of concrete, J. Build. Eng. 52 (2022) 104307, https://doi.org/10.1016/j.jobe.2022.104307.

[5] G.S. Simate, J. Cluett, S.E. Iyuke, E.T. Musapatika, S. Ndlovu, L.F. Walubita, A.E. Alvarez, The treatment of brewery wastewater for reuse: State of the art (jun 2011). doi:10.1016/j.desal.2011.02.035.

[6] L. Svarovsky, G. Svarovsky, Hydrocyclones, volume II (2013) 245.

[7] M.G. Farghaly, V. Golyk, G.A. Ibrahim, M.M. Ahmed, T. Neesse, Controlled wash water injection to the hydrocyclone underflow, Miner. Eng. 23 (4) (2010) 321–325, https://doi.org/10.1016/j.mineng.2009.09.021.

[8] K.J. Hwang, Y.W. Hwang, H. Yoshida, K. Shigemori, Improvement of particle separation efficiency by installing conical top-plate in hydrocyclone, Powder Technol. 232 (2012) 41–48, https://doi.org/10.1016/j.powtec.2012.07.059.

[9] L.F. Martínez, A.G. Lavín, M.M. Mahamud, J.L. Bueno, Vortex finder optimum length in hydrocyclone separation, Chem. Eng. Process. 47 (2) (2008) 192–199, https://doi.org/10.1016/j.cep.2007.03.003.

[10] Q. Yang, H.L. Wang, Y. Liu, Z.M. Li, Solid/liquid separation performance of hydrocyclones with different cone combinations, Sep. Purif. Technol. 74 (3) (2010) 271–279, https://doi.org/10.1016/j.seppur.2010.06.014.

[11] M. Ghodrat, S.B. Kuang, A.B. Yu, A. Vince, G.D. Barnett, P.J. Barnett, Numerical analysis of hydrocyclones with different conical section designs, Miner. Eng. 62 (2014) 74–84, https://doi.org/10.1016/j.mineng.2013.12.003.

[12] I. Mokni, H. Dhaouadi, P. Bournot, H. Mhiri, Numerical investigation of the effect of the cylindrical height on separation performances of uniflow hydrocyclone, Chem. Eng. Sci. 122 (2015) 500–513, https://doi.org/10.1016/j.ces.2014.09.020.

[13] S.S. Pathak, S. Mishra, M.H. Tyeb, A.K. Majumder, Spigot Design Modification to Alleviate Roping in Hydrocyclones, Min., Metall. Explor. 39 (2) (2022) 761–775, https://doi.org/10.1007/s42461-021-00503-x.

[14] N.K. Silva, D.O. Silva, L.G. Vieira, M.A. Barrozo, Effects of underflow diameter and vortex finder length on the performance of a newly designed filtering hydrocyclone, Powder Technol. 286 (2015) 305–310, https://doi.org/10.1016/j.powtec.2015.08.036.

[15] F.F. Salvador, M.A. Barrozo, L.G. Vieira, Filtering cylindrical–conical hydrocyclone, Particuology 47 (2019) 54–62, https://doi.org/10.1016/j.partic.2018.11.003.

[16] F.F. Salvador, G.G. Ascendino, É.V. de Faria, M.A.d.S. Barrozo, L.G.M. Vieira, Geometric optimization of filtering cylindrical hydrocyclones, Powder Technol. 381 (2021) 611–619, https://doi.org/10.1016/j.powtec.2020.12.036.

[17] L. Ma, Q. Yang, Y. Huang, P. Qian, J.G. Wang, Pilot Test on the Removal of Coke Powder from Quench Oil Using a Hydrocyclone, Chem. Eng. Technol. 36 (4) (2013) 696–702, https://doi.org/10.1002/ceat.201200316.

[18] Q. Yang, Z.M. Li, W.J. Lv, H.L. Wang, On the laboratory and field studies of removing fine particles suspended in wastewater using mini-hydrocyclone, Sep. Purif. Technol. 110 (2013) 93–100, https://doi.org/10.1016/j.seppur.2013.03.025.

[19] J. Lee, Practical applications of low-pressure hydrocyclone (LPH) for feed waste and fecal solid removal in a recirculating aquaculture system, Aquacult. Eng. 69 (2015) 37–42, https://doi.org/10.1016/j.aquaeng.2015.08.003.

[20] K. Sutherland, Oils and Hydraulic Systems, Filters and Filtration Handbook, Elsevier, 2008, pp. 295–367, https://doi.org/10.1016/b978-1-85617-464-0.00005-5.

[21] J.P. Li, X.J. Yang, L. Ma, Q. Yang, Y.H. Zhang, Z.S. Bai, X.C. Fang, L.Q. Li, Y. Gao, H.L. Wang, The enhancement on the waste management of spent hydrotreating catalysts for residue oil by a hydrothermal-hydrocyclone process, Catal. Today 271 (2016) 163–171, https://doi.org/10.1016/j.cattod.2015.08.037.

[22] K. Saengchan, A. Nopharatana, W. Songkasiri, Enhancement of tapioca starch separation with a hydrocyclone: effects of apex diameter, feed concentration, and pressure drop on tapioca starch separation with a hydrocyclone, Chem. Eng. Process. 48 (1) (2009) 195–202, https://doi.org/10.1016/j.cep.2008.03.014.

[23] E.C. Ramirez, D.B. Johnston, A.J. McAloon, W. Yee, V. Singh, Engineering process and cost model for a conventional corn wet milling facility, Ind. Crops Prod. 27 (1) (2008) 91–97, https://doi.org/10.1016/j.indcrop.2007.08.002.

[24] A.M. Van Dinther, C.G. Schroën, R.M. Boom, Separation process for very concentrated emulsions and suspensions in the food industry, Innovat. Food Sci. Emerg. Technol. 18 (2013) 177–182, https://doi.org/10.1016/j.ifset.2012.12.007.

[25] L. Hildebrandt, T. Zimmermann, S. Primpke, D. Fischer, G. Gerdts, D. Pröfrock, Comparison and uncertainty evaluation of two centrifugal separators for microplastic sampling, J. Hazard. Mater. 414 (2021) 125482, https://doi.org/10.1016/j.jhazmat.2021.125482.

[26] L. He, L. Ji, X. Sun, S. Chen, S. Kuang, Investigation of mini-hydrocyclone performance in removing small-size microplastics, Particuology 71 (2022) 1–10, https://doi.org/10.1016/j.partic.2022.01.011.

[27] O. González Pérez, J.M. Bisang, Electrochemical production of cobalt powder by using a modified hydrocyclone with ultrasonic assistance, Chemical Engineering and Processing -, Process Intensif. 168 (2021) 108560, https://doi.org/10.1016/j.cep.2021.108560.

[28] T.C. Rao, K. Nageswararao, A.J. Lynch, Influence of feed inlet diameter on the hydrocyclone behaviour, Int. J. Miner. Process. 3 (4) (1976) 357–363, https://doi.org/10.1016/0301-7516(76)90023-5.

[29] K. Nageswararao, D.M. Wiseman, T.J. Napier-Munn, Two empirical hydrocyclone models revisited, in: Minerals Engineering, Vol. 17, Pergamon, 2004, pp. 671–687. doi:10.1016/j.mineng.2004.01.017.

[30] C. Zhang, D. Wei, B. Cui, T. Li, N. Luo, Effects of curvature radius on separation behaviors of the hydrocyclone with a tangent-circle inlet, Powder Technol. 305 (2017) 156–165, https://doi.org/10.1016/j.powtec.2016.10.002.

[31] H. Liu, Q. Yin, Q. Huang, S. Geng, T. He, A. Chen, Experimental investigation on interaction of vortex finder diameter and length in a small hydrocyclone for solid-liquid separation, Sep. Sci. Technol. (Philadelphia) 57 (5) (2022) 733–748, https://doi.org/10.1080/01496395.2021.1936043.

[32] Q. Yang, H.L. Wang, J.G. Wang, Z.M. Li, Y. Liu, The coordinated relationship between vortex finder parameters and performance of hydrocyclones for separating light dispersed phase, Sep. Purif. Technol. 79 (3) (2011) 310–320, https://doi.org/10.1016/j.seppur.2011.03.012.

[33] S. Fu, Y. Qian, H. Yuan, Y. Fang, Effect of cone angles of a hydrocyclone for the separation of waste plastics with low value of density difference, Waste Manage. 140 (2022) 183–192, https://doi.org/10.1016/j.wasman.2021.11.028.

[34] Y. Liu, Q. Yang, P. Qian, H.L. Wang, Experimental study of circulation flow in a light dispersion hydrocyclone, Sep. Purif. Technol. 137 (2014) 66–73, https://doi.org/10.1016/j.seppur.2014.09.020.

[35] C. Zhang, B. Cui, D. Wei, S. Lu, Effects of underflow orifice diameter on the hydrocyclone separation performance with different feed size distributions, Powder Technol. 355 (2019) 481–494, https://doi.org/10.1016/j.powtec.2019.07.071.

[36] Y.N. Kyriakidis, D.O. Silva, M.A.S. Barrozo, L.G.M. Vieira, Effect of variables related to the separation performance of a hydrocyclone with unprecedented geometric relationships, Powder Technol. 338 (2018) 645–653, https://doi.org/10.1016/j.powtec.2018.07.064.

[37] A. Davailles, E. Climent, F. Bourgeois, A.K. Majumder, Analysis of swirling flow in hydrocyclones operating under dense regime, Miner. Eng. 31 (2012) 32–41, https://doi.org/10.1016/j.mineng.2012.01.012.

[38] L.R. Castilho, R.A. Medronho, Simple procedure for design and performance prediction of Bradley and Rietema hydrocyclones, Miner. Eng. 13 (2) (2000) 183–191, https://doi.org/10.1016/S0892-6875(99)00164-8.

[39] R.K. Dwari, M.N. Biswas, B.C. Meikap, Performance characteristics for particles of sand FCC and fly ash in a novel hydrocyclone, Chem. Eng. Sci. 59 (3) (2004) 671–684, https://doi.org/10.1016/j.ces.2003.11.015.

[40] I.C. Bicalho, J.L. Mognon, J. Shimoyama, C.H. Ataíde, C.R. Duarte, Separation of yeast from alcoholic fermentation in small hydrocyclones, Sep. Purif. Technol. 87 (2012) 62–70, https://doi.org/10.1016/j.seppur.2011.11.023.

[41] J. Izquierdo, R. Aguado, A. Portillo, J. Vicente, J. Bilbao, M. Olazar, Empirical Correlation for Calculating the Pressure Drop in Microhydrocyclones, Ind. Eng. Chem. Res. 57 (42) (2018) 14202–14212, https://doi.org/10.1021/acs.iecr.8b02258.

[42] K.-J. Hwang, Y.-W. Hwang, H. Yoshida, K. Shigemori, Improvement of particle separation efficiency by installing conical top-plate in hydrocyclone, Powder Technol. 232 (2012) 41–48, https://doi.org/10.1016/j.powtec.2012.07.059.

[43] L.F. Martínez, A.G. Lavín, M.M. Mahamud, J.L. Bueno, Vortex finder optimum length in hydrocyclone separation, Chem. Eng. Process. 47 (2) (2008) 192–199, https://doi.org/10.1016/j.cep.2007.03.003.

[44] L.-Y. Chu, W.-M. Chen, X.-Z. Lee, Effects of geometric and operating parameters and feed characters on the motion of solid particles in hydrocyclones, Sep. Purif. Technol. 26 (2–3) (2002) 237–246, https://doi.org/10.1016/S1383-5866(01)00171-X.

[45] J.J. Cilliers, S.T.L. Harrison, The application of mini-hydrocyclones in the concentration of yeast suspensions, Chem. Eng. J. 65 (1) (1997) 21–26, https://doi.org/10.1016/S1385-8947(96)03100-2.

[46] H. Wang, Y. Zhang, J. Wang, H. Liu, Cyclonic separation technology: Researches and developments, Chin. J. Chem. Eng. 20 (2) (2012) 212–219, https://doi.org/10.1016/S1004-9541(12)60381-4.

[47] Q. Yang, H.-L. Wang, Y. Liu, Z.-M. Li, Solid/liquid separation performance of hydrocyclones with different cone combinations, Sep. Purif. Technol. 74 (3) (2010) 271–279, https://doi.org/10.1016/j.seppur.2010.06.014.

[48] P. Bagdi, P. Bhardwaj, A.K. Sen, Analysis and Simulation of a micro hydrocyclone device for particle liquid separation, J. Fluids Eng.-Trans. Asme 134 (2). doi:10.1115/1.4006020.

[49] I.C. Bicalho, J.L. Mognon, J. Shimoyama, C.H. Ataíde, C.R. Duarte, Separation of yeast from alcoholic fermentation in small hydrocyclones, Sep. Purif. Technol. 87 (2012) 62–70, https://doi.org/10.1016/j.seppur.2011.11.023.

[50] M. Frachon, J.J. Cilliers, A general model for hydrocyclone partition curves, Chem. Eng. J. 73 (1) (1999) 53–59, https://doi.org/10.1016/S1385-8947(99)00040-6.

[51] K. Saengchan, A. Nopharatana, W. Songkasiri, Enhancement of tapioca starch separation with a hydrocyclone: effects of apex diameter, feed concentration, and pressure drop on tapioca starch separation with a hydrocyclone, Chem. Eng. Process. 48 (1) (2009) 195–202, https://doi.org/10.1016/j.cep.2008.03.014.

[52] M. Narasimha, A.N. Mainza, P.N. Holtham, M.S. Brennan, Air-core modelling for hydrocyclones operating with solids, Int. J. Miner. Process. 102–103 (2012) 19–24, https://doi.org/10.1016/j.minpro.2011.09.004.

[53] Y. Zhang, J. Ge, L. Jiang, H. Wang, Y. Duan, Effect of Internal Vortex-Finder on Classification Performance for Double Vortex-Finder Hydrocyclone, Separations 9 (4) (2022) 88, https://doi.org/10.3390/separations9040088.

[54] A. Davailles, E. Climent, F. Bourgeois, A.K. Majumder, Analysis of swirling flow in hydrocyclones operating under dense regime, Miner. Eng. 31 (2012) 32–41, https://doi.org/10.1016/j.mineng.2012.01.012.

[55] S.K. Kawatra, A.K. Bakshi, M.T. Rusesky, The effect of slurry viscosity on hydrocyclone classification, Int. J. Miner. Process. 48 (1–2) (1996) 39–50, https://doi.org/10.1016/s0301-7516(96)00012-9.

[56] G. Zhu, J.-L. Liow, Experimental study of particle separation and the fishhook effect in a mini-hydrocyclone, Chem. Eng. Sci. 111 (2014) 94–105, https://doi.org/10.1016/j.ces.2014.02.017.

[57] H. Schubert, On the origin of anomalous shapes of the separation curve in hydrocyclone separation of fine particles, Part. Sci. Technol. 22 (3) (2004) 219–234, https://doi.org/10.1080/02726350490501349.
[58] S. Pasquier, J.J. Cilliers, Sub-micron particle dewatering using hydrocyclones, Chem. Eng. J. 80 (1–3) (2000) 283–288, https://doi.org/10.1016/S1383-5866(00)00103-9.
[59] T. Ignatova, K. Mincheva, S. Ignatov, A. Dzhelyaydinova, T. Petkov, A. Kyazimov, Obtaining coarse dispersed kaolin for sanitary ceramics through hydrocycloning, J. Chem. Technol. Metall. 48 (2) (2013) 186–189.
[60] Q. Yang, H.L. Wang, J.G. Wang, Z.M. Li, Y. Liu, The coordinated relationship between vortex finder parameters and performance of hydrocyclones for separating light dispersed phase, Sep. Purif. Technol. 79 (3) (2011) 310–320, https://doi.org/10.1016/j.seppur.2011.03.012.
[61] M. Ghodrat, S.B. Kuang, A.B. Yu, A. Vince, G.D. Barnett, P.J. Barnett, Numerical analysis of hydrocyclones with different conical section designs, Miner. Eng. 62 (2014) 74–84, https://doi.org/10.1016/j.mineng.2013.12.003.
[62] I. Mokni, H. Dhaouadi, P. Bournot, H. Mhiri, Numerical investigation of the effect of the cylindrical height on separation performances of uniflow hydrocyclone, Chem. Eng. Sci. 122 (2015) 500–513, https://doi.org/10.1016/j.ces.2014.09.020.